EPJ B
Condensed Matter and Complex Systems
EPJ.org
your physics journal

Eur. Phys. J. B **81**, 441–449 (2011) DOI: 10.1140/epjb/e2011-20265-0

Intense laser field effect on impurity states in a semiconductor quantum well: transition from the single to double quantum well potential

C.A. Duque, M.E. Mora-Ramos, E. Kasapoglu, H. Sari and I. Sökmen

EDP SCIENCES
Società Italiana di Fisica
Springer

Eur. Phys. J. B **81**, 441–449 (2011)
DOI: 10.1140/epjb/e2011-20265-0

THE EUROPEAN PHYSICAL JOURNAL B

Regular Article

Intense laser field effect on impurity states in a semiconductor quantum well: transition from the single to double quantum well potential

C.A. Duque[1,a], M.E. Mora-Ramos[2], E. Kasapoglu[3], H. Sari[3], and I. Sökmen[4]

[1] Instituto de Física, Universidad de Antioquia, Calle 67 No. 53-108, A.A. 1226, Medellín, Colombia
[2] Facultad de Ciencias, Universidad Autónoma del Estado de Morelos, Ave. Universidad 1001, CP. 62209, Cuernavaca, Morelos, Mexico
[3] Cumhuriyet University, Physics Department, 58140 Sivas, Turkey
[4] Dokuz Eylül University, Physics Department, 35160 Buca, İzmir, Turkey

Received 2 April 2011 / Received in final form 2 May 2011
Published online 9 June 2011

Abstract. In this work are studied the intense laser effects on the impurity states in GaAs-$Ga_{1-x}Al_xAs$ quantum wells under applied electric and magnetic fields. The electric field is taken oriented along the growth direction of the quantum well whereas the magnetic field is considered to be in-plane. The calculations are made within the effective mass and parabolic band approximations. The intense laser effects have been included through the Floquet method by modifying the confinement potential associated to the heterostructure. The results are presented for several configurations of the dimensions of the quantum well, the position of the impurity atom, the applied electric and magnetic fields, and the incident intense laser radiation. The results suggest that for fixed geometry setups in the system, the binding energy is a decreasing function of the electric field intensity while a dual monotonic behavior is detected when it varies with the magnitude of an applied magnetic field, according to the intensity of the laser field radiation.

1 Introduction

The understanding of the effects of external electromagnetic fields on the optical and transport properties of low-dimensional systems – e.g., electrons confined in semiconductor nanostructures such as quantum wells (QWs), quantum-well wires (QWWs), and quantum dots (QDs) – is crucial for the evolution of the emerging nanoelectronics; an area that has attracted increasing interest due to the possibilities it opens in applied physics [1]. As it is well known, the application of either an electric or a magnetic field, and also of external perturbations like hydrostatic pressure or temperature, changes the quantum states of carriers confined in nanostructures [2]. Recently, the development of high-power tunable laser sources, such as free electron lasers, has fueled research activities on the interaction of intense laser fields with carriers in semiconductor nanostructures [3]. This has allowed the discovery of interesting physical phenomena. We can mention, for instance, the presence of changes in the electron density of states in QWs and QWWs [4–6], the measurement of zero-resistance states in two-dimensional electron gases under microwave radiation [7], terahertz resonant absorption in QWs [8], and Floquet-Bloch states in single-walled carbon nanotubes [9], among others.

The effect of an intense high-frequency laser field on the physical properties of bulk semiconductors has received some discussion and analysis in the literature [10–13]. More recently, a number of investigations have been published on the effect of the laser fields on low dimensional heterostructures [14–27]. Brandi et al. [14,15] extended the dressed atom approach to treat the influence of the laser field upon a semiconductor system. In the model, the interaction with the laser is taken into account through the renormalization of the semiconductor effective mass. More recently, Niculescu and Burileanu [16] have developed a theoretical study of the combined effects of intense high frequency laser and static magnetic fields on the binding and transition energies associated with the ground and some excited states of an on-center hydrogenic donor in a cylindrical GaAs QWW. They found that the effect of the laser field is more pronounced for s-like states, whereas for $2p$-like states the binding energy is weakly dependent on the laser dressing parameter. Using the same scheme, López et al. [17] have calculated the laser-dressing effects on the electron g-factor in GaAs-$Ga_{1-x}Al_xAs$ QWs and QWWs under applied magnetic fields. Their work indicates the possibility of manipulating and tuning the

[a] e-mail: cduque_echeverri@yahoo.es

conduction-electron g-factor in heterostructures by changing the detuning and laser field intensity.

On the other hand, the intense laser field effects on the density of impurity states of shallow donors in a square, V-shaped, and inverse V-shaped QWs have been studied by Niculescu et al. [21,22] and concluded that a proper consideration of the density of impurity states may be relevant in the interpretation of the optical phenomena related to shallow impurities in QWs; where the effects of an intense laser field compete with the applied electric field and the quantum confinement. The laser effects have also been included in calculations of a donor-impurity polarizability in a QW under an applied electric field, finding that the polarizability is a non monotonic function of the external perturbations like the applied electric field and the incoming laser radiation [23]. A theoretical study from Lima et al. [28] reveals the appearance of an unexpected transition from single to double QW potential induced by intense laser fields in a semiconductor QW. Within the laser-dressed potential model these authors found the formation of a double-well potential for laser frequencies and intensities such that the so-called laser-dressing parameter α_0 is larger than $L/2$, where L is the QW width. This fact creates the possibility of generating resonant states into the channel and of controlling the population inversion in QW lasers operating in the optical pumping scheme. Finally, the study of intense laser field effects has been extended to another heterostructures such as QWWs and QDs with several configurations of the quantum confinement, stoichiometry of the well and barrier regions, geometries of the systems, and external perturbations like applied electric and magnetic fields and hydrostatic pressure [24–27].

The influence of the impurities in optical and electronic properties of semiconducting heterostructures is a subject of relevance in the physics of those systems due to the changes in the electron energy states induced by their presence. In consequence, it is arguably of interest the study of the impurity states in confined semiconductor structures under the effects of intense laser fields, given that they reveal some non-linear optical properties of such systems, related with the electron spectrum. For these reasons, the present work is concerned with the theoretical study of the effects of intense laser fields on the impurity states in single QWs under the combined influence of the electric field applied through the growth direction and the magnetic field applied in-plane. The laser-dressed potential above mentioned, as well as the effect of single-to-double potential well transition are the subject of particular investigation in our case. The paper is organized as follows. In Section 2 we describe the theoretical framework. Section 3 is dedicated to the results and discussion, and finally, our conclusions are given in Section 4.

2 Theoretical framework

Here we are concerned with intense laser effects on the binding energy of a donor impurity in a single GaAs-$Ga_{1-x}Al_xAs$ QW grown along the z-axis and in the presence of crossed electric and magnetic fields. The present theoretical approach assumes the envelope-function and parabolic-band approximations. We choose the electric field along the growth direction, $\vec{F} = (0, 0, -F)$. The magnetic field is in-plane-oriented, taken along the x-direction, $\vec{B} = (B, 0, 0)$, and the Landau gauge $\vec{A}(\vec{r}) = (0, -B\,z, 0)$ is used. Then, the Hamiltonian for the confined electron takes the following form [29–31]

$$\hat{H} = \frac{1}{2\,m_e^*}\left(\hat{\vec{p}} + \frac{e}{c}\vec{A}\right)^2 + V(z) - e\,F\,z\, - \frac{e^2}{\varepsilon\,|\vec{r} - \vec{r_0}|}, \quad (1)$$

where $\vec{A} = \vec{A}(\vec{r})$ and $\hat{\vec{p}}$ are the vector potential and momentum operator, respectively, $\vec{r} = (\vec{\rho}, z)$ is the electron coordinate ($\vec{\rho} = (x, y)$ is the in-plane electron coordinate), $\vec{r_0} = (0, z_0)$ is the impurity position, m_e^* is the electron effective mass, ε is the static dielectric constant, e is the absolute value of the electron charge, and $V(z)$ is the QW confining potential (where $V(z) = 0$ for $|z| \leq L/2$ and $V(z) = V_0$ for $|z| > L/2$). The electron effective mass and the static dielectric constant have been considered the same as in GaAs throughout the GaAs-$Ga_{1-x}Al_xAs$ QW.

In order to find the eigenfunctions $\Psi(\vec{r})$ of the electron Hamiltonian (Eq. (1)), it is important to notice that the in-plane electron momentum is an exact integral of motion [29–31] and the electron wave function may be written as

$$\Psi\left(\vec{\boldsymbol{r}}\right) = \frac{\exp\left[(i/\hbar)\left(p_x x + p_y y\right)\right]}{\sqrt{S}}\,\Phi(\rho, z), \quad (2)$$

where S is the transverse area of the GaAs-$Ga_{1-x}Al_xAs$ QW and $\vec{p} = (p_x, p_y)$ is the eigenvalue of the operator $\hat{\vec{p}}$. If $\vec{p} = 0$ (ground state), $\Phi(\rho, z)$ is the eigenfunction of the Hamiltonian

$$\hat{H} = \frac{\widehat{p}_z^{\,2}}{2\,m_e^*} + V(z) + \frac{1}{2}m_e^*\,\omega^2\,z^2 - e\,F\,z - \frac{e^2}{\varepsilon\left[\rho^2 + (z - z_0)\right]^{\frac{1}{2}}}, \quad (3)$$

where $\omega = e\,B/(m_e^*\,c)$, is the cyclotron frequency. We adopt the variational scheme used by Fox et al. [32] and Galbraith and Duggan [33] which consists of minimizing the functional

$$E(\lambda) = \langle \Phi(\rho, z)|H|\Phi(\rho, z)\rangle \quad (4)$$

using the variational wave functions as

$$\Phi(\rho, z) = N\,\phi(z)\,\exp\left(-\lambda\,|\vec{r} - \vec{r_0}|\right), \quad (5)$$

where λ is the variational parameter and N the normalization constant. Here we follow the work of Xia and Fan [34] and we write $\phi(z)$ as an expansion of the type

$$\phi(z) = \left(\frac{2}{L_\infty}\right)^{\frac{1}{2}} \sum_{m=1}^{\infty} C_m\,\sin\left(\frac{m\pi z}{L_\infty} + \frac{m\pi}{2}\right). \quad (6)$$

In the present work we have taken 200 terms in equation (4). L_∞ (=500 Å in this work) corresponds to

$$\langle V\rangle(z,\alpha_0) = \frac{V_0}{\pi} \times \begin{cases} \pi, & -\infty < z \leq -L/2 - \alpha_0, \\ \arccos\left(\frac{L/2+z}{\alpha_0}\right), & -L/2 - \alpha_0 < z \leq -L/2 + \alpha_0, \\ 0, & -L/2 + \alpha_0 < z \leq +L/2 - \alpha_0, \\ \arccos\left(\frac{L/2-z}{\alpha_0}\right), & +L/2 - \alpha_0 < z \leq +L/2 + \alpha_0, \\ \pi, & +L/2 + \alpha_0 < z \leq +\infty, \end{cases} \tag{7}$$

$$\langle V\rangle(z,\alpha_0) = \frac{V_0}{\pi} \times \begin{cases} \pi, & -\infty < z \leq -L/2 - \alpha_0, \\ \arccos\left(\frac{L/2+z}{\alpha_0}\right), & -L/2 - \alpha_0 < z \leq +L/2 - \alpha_0, \\ \pi + \arcsin\left(\frac{z-L/2}{\alpha_0}\right) - \arcsin\left(\frac{z+L/2}{\alpha_0}\right), & +L/2 - \alpha_0 < z \leq -L/2 + \alpha_0, \\ \arccos\left(\frac{L/2-z}{\alpha_0}\right), & -L/2 + \alpha_0 < z \leq +L/2 + \alpha_0, \\ \pi, & +L/2 + \alpha_0 < z \leq +\infty. \end{cases} \tag{8}$$

the length of the QW, with rigid walls, used to expand the $\phi(z)$ wave function. With these values of the number of terms in the sum of equation (6) and the size of the infinite quantum well, the convergence of the lowest eigenvalue associated to the $f(z)$ function is ensured until 10^{-3} meV.

In order to consider the intense laser effects (ILF) (the polarization of the laser radiation is parallel to the z-direction), we have followed the Floquet method [35,36]. Consequently, the second term at the right hand side in equation (3) must be replaced by $V(z) \to \langle V\rangle(z,\alpha_0)$ where for $\alpha_0 \leq L/2$

see equation (7) *above,*

and for $\alpha_0 > L/2$

see equation (8) *above.*

Here

$$\alpha_0 = (e\,A_0)\,/\,(m_e^*\,c\,\omega) = \left(I^{1/2}/\omega^2\right)(e/m_e^*)\,(8\,\pi/c)^{1/2} \tag{9}$$

is the laser-dressing parameter (from now on ILF-parameter) [37]. In equation (7), I and ω are, respectively, the average intensity and the frequency of the laser, c is the velocity of the light, and A_0 is the amplitude of the vector potential associated with the incident radiation.

Under the laser effects the last term of equation (3) – the one-center electron-impurity Coulomb interaction – must be replaced by two centers Coulomb interaction as

$$\langle V\rangle_C(z,\alpha_0) = -\frac{e^2}{2\,\varepsilon\left[\rho^2 + (z - z_0 - \alpha_0)^2\right]^{1/2}} - \frac{e^2}{2\,\varepsilon\sqrt{\rho^2 + (z - z_0 + \alpha_0)^2}}. \tag{10}$$

Extended details about dressed potential in equations (7), (8), and (10) and the nonperturbative theory developed to describe the atomic behavior in intense high frequency laser field can be found in references [18,28,38].

3 Results and discussion

In this section, we present the numerical results for the intense laser effects on the non-correlated electron ground state energy and donor impurity binding energy in single QW under crossed growth direction applied electric field and in-plane applied magnetic field. For the applied electric field values reported in this study – less than 100 kV/cm – the first calculated electron state is a stationary one.

We take the case of a GaAs-$Ga_{0.67}Al_{0.33}As$ single QW as a prototypical system. For the potential that confines the electrons inside the well regions, we choose a 60% of the barrier-well bandoffset [$V_e = 0.6\,(1155\,x + 370\,x^2)$ meV, where x is the Aluminum concentration in the barrier material]. The parameters used in our calculations are [29]: $m_e^* = 0.0665\,m_0$ (where m_0 is the free electron effective mass) and $\varepsilon = 12.35$.

In Figure 1 we present the amplitude of probability for the ground state of a confined electron in a GaAs-$Ga_{0.67}Al_{0.33}As$ QW as a function of the z-coordinate. The results are for $L = 100$ Å with two values of the ILF-parameter and for three different setups of the applied electric and magnetic fields.

One can observe the following features: the renormalization of the QW potential due to the ILF effects leads to the variation of the effective well width. Within the range of $\alpha_0 \leq L/2$, it can be noticed that when the energy is below that of the inflexion point of the potential profile, there is a reduction of the well width which, in the case of the well bottom energy follows the law $L' = L - \alpha_0/2$. On the other hand, for energies above the one corresponding to the potential barrier inflexion point, the QW width enhances, with a limiting value of $L' = L + \alpha_0/2$, which

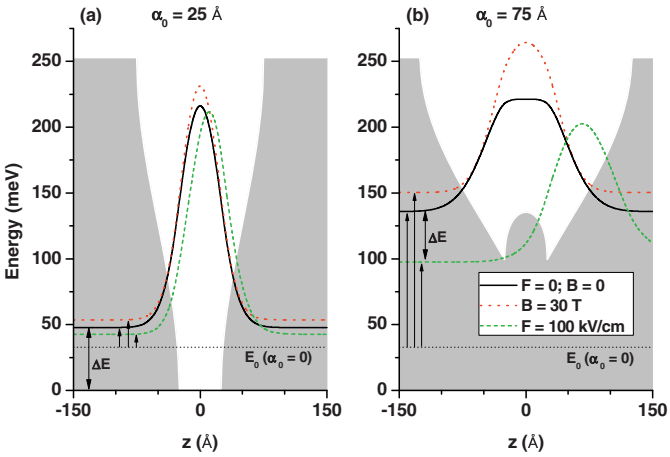

Fig. 1. (Color online) The amplitude of probability for the ground state of a confined electron in a GaAs-$Ga_{0.67}Al_{0.33}As$ QW as a function of the z-coordinate. The results are for $L =$ 100 Å and two different values of the ILF-parameter: $\alpha_0 =$ 25 Å (a) and $\alpha_0 = 75$ Å (b). Solid lines are for $F = 0$ and $B =$ 0, dotted lines are for $F = 0$ with $B = 30$ T, and dashed lines are for $F = 100$ kV/cm with $B = 0$. The horizontal dotted line corresponds to the energy of the ground state for the confined electron in the GaAs-$Ga_{0.67}Al_{0.33}As$ QW at $\alpha_0 = 0$. The zero of the each amplitude of probability curve is localized in the eigenenergy of the each eigenstate.

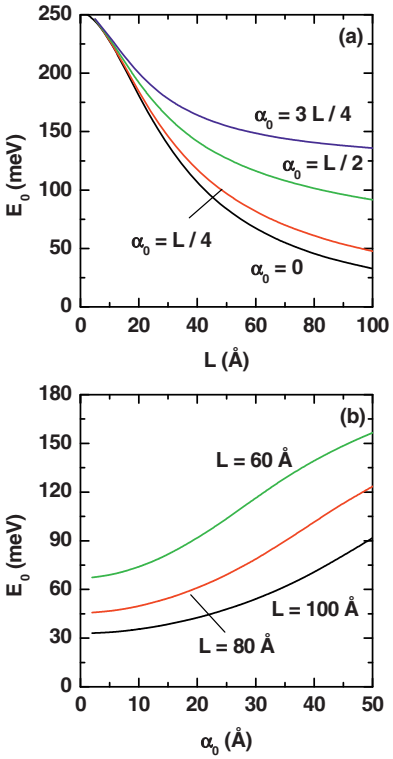

Fig. 2. (Color online) Ground state energy of a confined electron in a GaAs-$Ga_{0.67}Al_{0.33}As$ QW as a function of the well-width, for several values of the ILF-parameter (a), and as a function of the ILF-parameter, for several values of the the well-width (b). In both figures, $F = 0$ and $B = 0$.

corresponds to the energy of the potential barrier top. This potential profile deformation has the consequence of an increasing of the electron confinement, driven by the increment of α_0, when the energy of the electron ground state is below the half-height of the QW. At the same time, it implies a decreasing in the electron confinement with growing laser-dressing parameter if the ground electron energy is above the half-height of the well. As $\alpha_0 > L/2$, the energy of the electron ground state continues to augment. This does not mean that the confinement keeps a growing path. In fact, it should be noticed that this energy increasing is basically due to the displacement of the potential well bottom towards higher values of the energy. However, when comparing Figures 1a and 1b it is observed that the energy of the lowest confined state, with respect to the bottom of the QW, has gone from 47.72 meV in Figure 1a to 37.26 meV in Figure 1b – see the arrows denoted as ΔE in Figures 1a and 1b – which actually represents an effective decreasing of the electron confinement associated to the effective widening of the QW. For $\alpha_0 = 75$ Å the ground state energy of the electron essentially coincides with the maximum of the central "potential hill" in the – now double – well profile. This is also manifested in the flat dependence shown by the top of the curve corresponding to its density of probability. Then, for even larger values of α_0 the ground state will lie below the energy position of that central potential maximum. In consequence, we shall have an electron confined within a system with two strongly coupled potential wells. In a given case in which α_0 is further increased, a situation with the two completely uncoupled QW should be reached, and the energy of the ground state will become twofold degenerate.

In Figure 2, the calculations for the ground state energy of a confined electron in a single GaAs-$Ga_{0.67}Al_{0.33}As$ QW as a function of the well-width are presented for several values of the ILF-parameter, (a); and (b) as a function of the ILF-parameter, for several values of the well-width, for zero applied electric and magnetic field.

As long as L augments, the potential barrier confinement effects on electrons clearly decrease. Hence, the value of E_0 diminishes as can be seen in Figure 2a – for all the considered α_0-values. There, it is readily apparent that in the limit of $L = 0$ all curves go towards the same value $E_0 = V_0$. Notice that in such limit the results are independent of the ILF-parameter. It is also readily observed that the influence of the ILF-parameter becomes important starting from $L \approx 20$ Å. For a fixed value of L, say $L = 50$ Å, E_0 is a growing function of the magnitude of α_0. In the region $\alpha_0 \leq L/2$, this increment is due to the decreasing of the effective width of the QW bottom. For $\alpha_0 > L/2$, the increasing of E_0 is essentially due the displacement of the potential bottom towards higher energy values. However, in the case of $\alpha_0 > L/2$, and given that the potential well barrier had a fixed a value in the situation without laser field applied, there will be an effective decreasing of the height of the confining potential barrier – the height of the barrier including

the laser effects, when $\alpha_0 > L/2$, has an approximate height of de $E = \frac{2\,V_0}{\pi}\,\arcsin(\frac{L}{2\,\alpha_0})$. It is also seen that at $L = 100$ Å – right-hand side of Figure 2a – the curves depicted have four distinct tendencies towards very different values of the energy. The curve for $\alpha_0 = 0$ corresponds to an electron confined within a QW which has V_0 potential height and width of 100 Å and which bottom is located at $E = 0$. The curve $\alpha_0 = L/4$ tends to the limit of a QW of width equals to 50 Å and potential barrier of height V_0 measured from the zero energy as well. The curve corresponding to $\alpha_0 = L/2$ tends towards the limit value for a QW of 200 Å of width with barrier height given by V_0; also measured from the zero energy. Finally, the curve with $\alpha_0 = 3L/4$ approaches the limit corresponding to a 250 Å wide QW with a potential barrier height approximately equals to $V_0/2$, measured from the value $E = \frac{V_0}{\pi}\,[\pi - 2\,\arcsin(\frac{L}{2\,\alpha_0})]$.

In Figure 2b it is shown the growing character of E_0 as a function of the ILF-parameter. We considered three distinct values of the QW width. It can be observed that as long as the QW width decreases, the effects of α_0 become more evident. An increment from zero to 50 Å of the ILF-parameter means an increment of ∼60 meV in the case $L = 100$ Å; of ∼80 meV if $L = 80$ Å; and of ∼90 meV for $L = 60$ Å. This strengthening of the laser field effects is closely related to the "unique" value of E_0 taken by all the curves in Figure 2a when $L = 0$, and also to the shifting upwards suffered by the energy of the QW bottom, when $\alpha_0 > L/2$.

In Figure 3 the results for the binding energy of on-center donor impurity in a GaAs-$Ga_{0.67}Al_{0.33}As$ QW as a function of the well-width, are depicted for several values of the ILF-parameter (Fig. 3a), and as a function of the ILF-parameter, for several values of the the well-width (Fig. 3b). In both figures, $F = 0$ and $B = 0$.

Let us look first at Figure 3a. First, notice that for $L = 0$ all the binding energy curves converge towards the same value $E_b = 7.21$ meV. This energy is 20% higher than the effective Rydberg in GaAs – 5.97 meV. This can be explained by remembering that according to the setup of our model potential, the condition $L = 0$ implies a situation in which we have a single electron bound to an impurity placed at the center of an infinite-barrier QW of $L_\infty = 500$ Å width. Same as Figure 2, it is clear that according to the way all these curves have been parameterized by means of the ILF-parameter, the results for them must coincide if $L = 0$. The behavior exhibited by the curve corresponding to $\alpha_0 = 0$ has been widely reported in the literature. When $L \to 0$ one has an electron bound to an impurity in a $Ga_{0.67}Al_{0.33}As$ infinite-barrier QW of width 500 Å; and in the case of $L \to 500$ Å – not depicted in Figure 3a –, we face the problem of an electron bound to an impurity in a GaAs infinite-barrier QW of width 500 Å. It is clear that in our model and when $\alpha_0 = 0$, the binding energy for on-center donor impurity must be the same in the two limits: for $L \to 0$ and for $L \to 500$ Å. When $\alpha_0 = 0$ and $L = 100$ Å there exists a strong localization of the electron wave function in the GaAs QW region. For that reason, at this value of the QW-width the binding energy has a substantially larger value in comparison with $L = 0$.

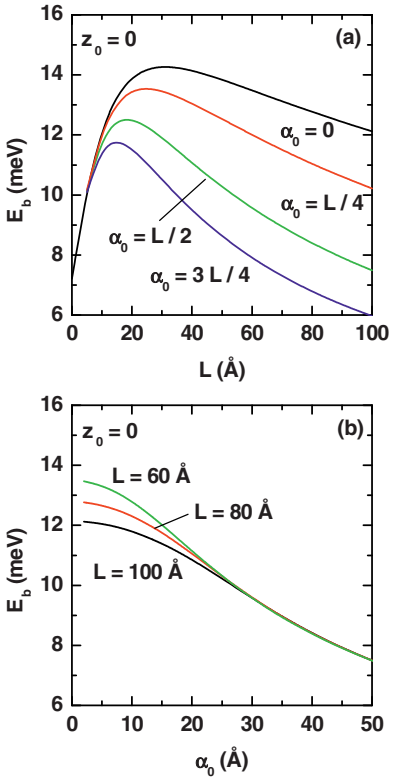

Fig. 3. (Color online) Binding energy of on-center donor impurity in a GaAs-$Ga_{0.67}Al_{0.33}As$ QW as a function of the well-width, for several values of the ILF-parameter (a), and as a function of the ILF-parameter, for several values of the the well-width (b). In both figures, $F = 0$ and $B = 0$.

We must notice that for finite QW widths ($L > 0$), E_b is always a decreasing function of the ILF-parameter. Let us see in more detail what happens: taking a fixed value of L, say $L = 100$ Å, when $\alpha_0 = 0$ one has an electron confined in a QW of width $L = 100$ Å with an impurity at the center of the well. In that case, the impurity position exactly coincides with the space region where the electron density of probability has a maximum. Therefore, there will be a small value for the expected electron-impurity distance with the consequent large value of the binding energy. If we now have $\alpha_0 = L/4$, in accordance with Figure 2a, it is detected an increasing of the localization of the electron probability density around the center of the QW. But in this case, the problem corresponds to that of an electron bound to two Coulombic centers localized at $z = \pm\alpha_0 = \pm L/4$, each with a charge magnitude of $e/2$ – see equation (8). In consequence, this is equivalent to an augment of the expected value of the electron-impurity distance with the corresponding diminishing in the binding energy. In this situation the Coulombic interaction decreases and this phenomenon is dominant over the increment in the carrier slocalization. In accordance, although the second effect would imply an augment in E_b, the overall result is, in fact, its decreasing.

Considering the case where $\alpha_0 = L/2$, it is possible to detect a weakening of the electron localization around the center of the heterostructure since the problem is – now – actually that of an electron confined in a QW of width 200 Å and potential barrier of V_0. Indeed, the maximum of the electron density of probability still lies at the center of the structure. But in this case, the two Coulomb centers with charge $e/2$ are located at $z = \pm\alpha_0 = \pm L/2$, which corresponds to the position of the walls of the real QW (with no laser effects). Again, the binding energy keeps decreasing because both effects are additive: (1) the binding energy decreases due to the loss of localization in the wave function, (2) E_b diminishes because of the augment of the expected value for the distance between the electron and the two Coulomb-centers.

Finally, when $\alpha_0 = 3L/4$ the situation is that the carrier localization around the central region of the QW decreases, in accordance with what can be observed from solid line in Figure 1b. This implies an augment of the electron localization towards the well barrier regions, which are approximately located at $z = \pm 5L/4$, and have an approximate height given by $E = \frac{2\,V_0}{\pi}\,\arcsin(\frac{L}{2\,\alpha_0})$. This results in a additional diminishing of the carrier localization as well as of the binding energy. Besides, both $e/2$-charge centers are now located in the $Ga_{0.67}Al_{0.33}As$ region, at the positions $z = \pm\alpha_0 = \pm 3L/4$ where, according to Figure 1b the electron density of probability essentially approaches zero. For this reason the expected value of the distance between the electron an both Coulombic centers will be significantly large, with the consequent falling observed in the values of E_b, such as it is shown in Figure 3a.

In Figure 3b the results of the curve marked with the label $L = 100$ Å correspond to the already discussed behavior for such a well width which can be observed at the right end of Figure 3a. That is the binding energy diminishes as long as the value of the ILF-parameter grows, as a result of the augment of the electron-impurity distance (when $\alpha_0 < 50$ Å), and of the combined effect of this distance augment and of the reduction in electron localization (when $\alpha_0 > 50$ Å). In the limit $\alpha_0 \to 0$, it is observed that the binding energy grows as long as the QW width decreases. That is, for smaller widths the carrier localization in the central region of the QW – where the impurity is precisely placed – becomes larger. Small increments of the ILF-parameter, $\alpha_0 < 30$ Å, keep this growing character for E_b, while the well width decreases. This shows that for such small values of the laser parameter, the contribution coming from the well-width-related values of the carrier localization is dominant over that of the ILF-parameter. On the other hand, for $\alpha_0 > 30$ Å, it can be seen that the laser effects become dominant for the binding energy, in comparison with the influence that the changes in QW size have over it. This is noticed from the fact that all curves overlap, which is a consequence of the rather high increasing of the electron-impurity distance due to the penetration of the Coulomb centers into the $Ga_{0.67}Al_{0.33}As$ region, where the electron amplitude of probability is essentially null.

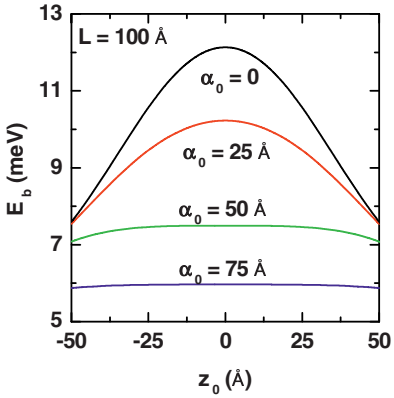

Fig. 4. (Color online) Binding energy of a donor impurity in a GaAs-$Ga_{0.67}Al_{0.33}As$ QW as a function of the impurity position and for several values of the ILF-parameter. The results are for $L = 100$ Å, $F = 0$, and $B = 0$.

Figure 4 depicts our results for the binding energy of a donor impurity in a GaAs-$Ga_{0.67}Al_{0.33}As$ QW as a function of the impurity position and for several values of the ILF-parameter. The results are for $L = 100$ Å, $F = 0$, and $B = 0$. Given that this figure is constructed for $F = 0$, the symmetry of reflection – with respect to the plane $z = 0$ – of the binding energy curves is clearly exhibited. The origin of the coordinates have been taken to be at the center of the QW. For that reason, moving the impurity along the $+z$ direction has the same effects that the equivalent displacement towards $-z$. From Figure 1 it is possible to observe also the symmetric character of the carrier confinement. The result for $\alpha_0 = 0$ has been widely reported in the literature: the binding energy decreases symmetrically as long as the position of the impurity approaches the potential barriers. This is a consequence of the repulsion of the wave function due precisely to the presence of the barriers, with an increment of the electron-impurity distance, thus leading E_b to have smaller values. A second way of viewing this situation is by realizing that with the maximum of the probability density located at the QW center, the displacement of the impurity position towards the barriers implies the increasing of the electron-impurity distance. This leads to the weakening of the electrostatic interaction. Hence, the decreasing in value of E_b. This behavior is kept for growing values of the ILF-parameter. However, the larger α_0 is, the less noticeable turns the impurity displacement towards the QW barriers. The reason for that is that making the ILF-parameter to be large enough (for instance $\alpha_0 = 75$ Å in a QW of width $L = 100$ Å) provokes that the electron wave function is distributed in a quasi-constant manner over the region in which the impurity is moving: $|z_0| \leq 50$ Å, resulting in non significant changes in the binding energy.

In Figure 5, the calculated ground state energy of a confined electron (a) and the binding energy of on-center donor impurity (b) in a GaAs-$Ga_{0.67}Al_{0.33}As$ QW are found, as functions of the applied electric field, for two fixed values of the ILF-parameter. The results presented are obtained for $L = 100$ Å with $B = 0$.

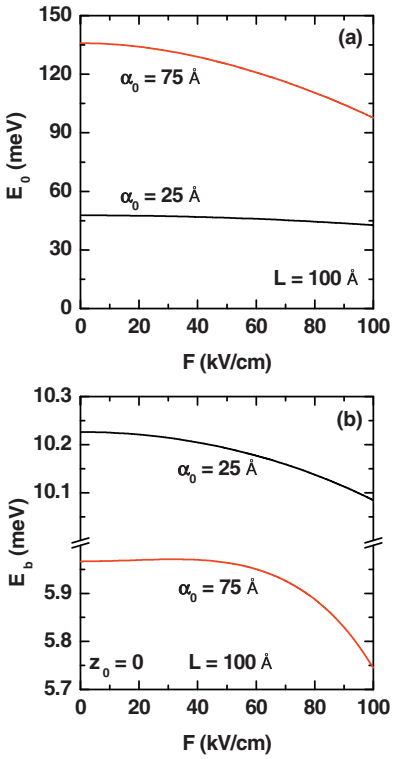

Fig. 5. (Color online) Ground state energy of a confined electron (a) and binding energy of on-center donor impurity (b) in a GaAs-$Ga_{0.67}Al_{0.33}As$ QW as a function of the applied electric field and for two values of the ILF-parameter. In both figures, $L = 100$ Å and $B = 0$.

As it has been already explained in the discussion of Figure 1, in the case of a QW of width $L = 100$ Å, when $\alpha_0 = 25$ Å, the system essentially behaves like a QW of width 50 Å with a strong wave function localization around $z = 0$. If we have $\alpha_0 = 75$ Å, then it would correspond to a QW with $L = 250$ Å and barrier height given by $E = \frac{2\,V_0}{\pi}\,\arcsin(\frac{L}{2\,\alpha_0})$, with a weaker wave function localization around $z = 0$. Naturally, in the first of these cases the system is much less sensitive to the electric field effects, as can be seen by comparing the curves in Figure 5a. The decreasing behavior of the ground state energy, E_0, as a function of the electric field is explained by the reduction in the effective potential barrier height which is located at $z = L/2 + \alpha_0$. This barrier height decreases according with the functional form $V = V_0 - e\,F\,(L/2 + \alpha_0)$. This reduction implies a diminishing of the wave function localization near $z = 0$ and, consequently, results in a decreasing of E_0 for growing electric field intensities.

If we now introduce the effects of the impurity in the system (Fig. 5b), the two $e/2$ Coulombic charge centers located at $z = \pm\alpha_0$ will act in such a way that an additional carrier confinement is provided. We have already explained what happens to the binding energy for $F = 0$ when the ILF-parameter is increased. But when $F \neq 0$, the electric field favors a reduction in the average distance between the Coulombic center located at the point $z = +\alpha_0$ and the maximum of the electron wave function whilst the distance with respect to the Coulombic center located at $z = -\alpha_0$ augments. Then, the system goes from being an electron bound to a couple of electrostatic centers to that of an electron bound to a single Coulombic center with charge $e/2$. This situation is clearly associated with a the lowering of the binding energy.

There are quite marked differences between the two curves in Figure 5b. The curve with $\alpha_0 = 25$ Å exhibits a weaker dependence with the electric field whereas the curve corresponding to the laser parameter $\alpha_0 = 75$ Å shows a quasi-constant behavior until $F = 40$ kV/cm, and then starts to rapidly decrease for higher values of the field intensity. This can be explained with the help of the following reasons: first, in the case $\alpha_0 = 25$ Å, the considered electric field values are not capable of inducing a displacement of the wave function maximum from the center of the well, such as is observed from Figure 1a when one compares the curve for $F = B = 0$ and the curve in which $F = 100$ kV/cm and $B = 0$. So, this implies that the changes in the distance between the electron and the Coulomb centers are not really significant. Besides, given that in the case of $\alpha_0 = 75$ Å the effective width of the QW is of the order of 250 Å, when $F > 40$ kV/cm, the electric field strength is capable of inducing a shift of the probability density maximum towards the barrier region, where the impurity is precisely placed. The distance between the electron and the impurity center located at $z = 75$ Å is therefore reduced. It should be also noticed that for this later magnitude of the ILF-parameter, the confining potential has suffered a decreasing due to the appearance of the central maximum in the function $\langle V\rangle(z, \alpha_0)$ which originates the formation of the pair of coupled quantum wells. The presence of these two wells is manifested in the flat top of the dependence of the probability density curve in Figure 1b for zero fields. The quasi-constant behavior of the binding energy within the field strength range of $F < 40$ kV/cm, when $\alpha_0 = 75$ Å is explained by the fact that although there is a weakening of the interaction between the electron and the two Coulomb centers, the presence of the electric field allows to confine the charge carriers within the QW that is formed in the region $0 < z < L/2$ – see Figure 1b. This originates an augment in the carrier localization and, as a result of it, of the binding energy. We then have two competing effects that give the resultant behavior above mentioned.

In Figure 6 we present the ground state energy of a confined electron (a) and the binding energy of on-center donor impurity (b) in a GaAs-$Ga_{0.67}Al_{0.33}As$ QW as a function of the applied magnetic field, for two different values of the ILF-parameter. In both figures, $L = 100$ Å and $F = 0$.

Figure 6a clearly allows us to observe that E_0 augments as a consequence of the increment in the magnetic field strength. Again, this happens because as long as B increases there will be a greater localization of the carriers in the vicinity of $z = 0$. It is worth noticing that when $\alpha_0 = 25$ Å the variations in E_0 are quite small since the system itself is already strongly confined given the reduced

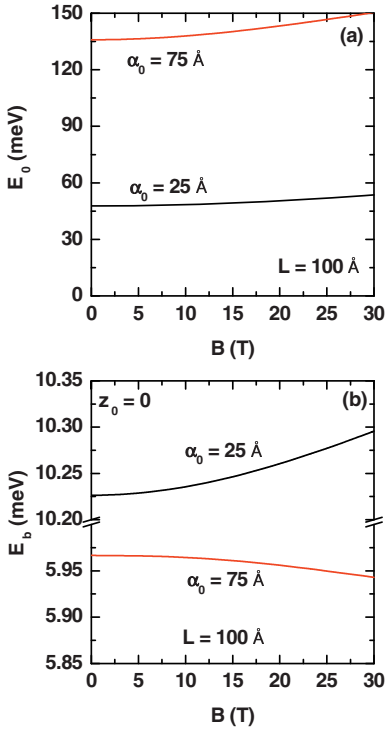

Fig. 6. (Color online) Ground state energy of a confined electron (a) and binding energy of on-center donor impurity (b) in a GaAs-$Ga_{0.67}Al_{0.33}As$ QW as a function of the applied magnetic field and for two values of the ILF-parameter. In both figures, $L = 100$ Å and $F = 0$.

effective size of the QW width. In the case of $\alpha_0 = 75$ Å, it is clear that the effective well has a much larger width, and the potential barriers have a much smaller height. Then the system becomes more sensitive to the external perturbations that induce quantum confinement, such as the applied magnetic field.

The analysis of Figure 6b allows to observe two opposite effects of the applied magnetic field on the binding energy, depending on the magnitude of the ILF-parameter. In the case of $\alpha_0 = 25$ Å, the binding energy grows with B, whilst for $\alpha_0 = 75$ Å, E_b decreases when the magnetic field strength augments. Let us discuss this phenomenon in more detail. For $\alpha_0 = 25$ Å and at zero magnetic field, the maximum of the electron probability density is in the region close to $z = 0$. When a finite intensity field is applied, the density of probability is reinforced over the same region, making the system to be more confined. This causes the increasing of the binding energy.

Now, when $\alpha_0 = 75$ Å, the presence of a potential barrier in the region around $z = 0$ causes the confinement of the electron system to be mainly located in the ILF-induced two-well region, which manifests trough the flatness of the maximum of the probability density, as seen from Figure 1b. The application of the magnetic field provokes the strengthening of the wave function maximum in the region around $z = 0$. This is observed in the curve corresponding to $F = 0$ and $B = 30$ T of Figure 1b. As a consequence, there is an augment of the distance between the carriers and the two Coulomb centers located at $\alpha_0 = \pm 75$ Å, which leads to a decreasing of the Coulombic correlation and, therefore, to a reduction of the binding energy.

4 Conclusions

In this work we have studied the intense laser effects on the binding energy of a donor impurity in GaAs-$Ga_{1-x}Al_xAs$ quantum wells under the influence of applied electric and magnetic fields. The calculations were performed within the effective mass and parabolic band approximations. The intense laser effects have been included through the Floquet method in the confinement potential associated to the heterostructure. The findings can be summarized as follows.

For zero applied field, the ground state energy of the electron confined in the quantum well is a decreasing function of the well width for every intensity of the laser field. If the width of the QW remains fixed, then the ground state energy is a growing function of the ILF-parameter. Under the same conditions, the on-center impurity binding energy diminishes as a function of the ILF-parameter for all the values of the well width considered. The same quantity shows a mixed character when it is considered as a function of the QW width for different values of α_0: for smaller widths, E_b is an increasing function of L whereas it becomes a decreasing function of the well width when L adopts larger values.

If E_b is considered a function of the position of the impurity atom, it is found that the binding energy is a symmetrical function with a well defined maximum for the impurity at the QW center and decreasing for larger values of $|z_0|$, in the situation of fixed QW width and small values of the ILF-parameter. When α_0 increases, this maximum becomes less pronounced and the dependence is becoming almost a constant.

If only an electric field is applied to the system, it is detected that keeping fixed both the impurity position (at the center) and the quantum well width, the impurity binding energy is a decreasing function of the field intensity for all – finite – values of the ILF-parameter, with a steepest rate of diminishing for large F when α_0 is larger. On the other hand, if there is only a magnetic field applied, for the fixed configuration above commented, it is found a dual behavior of E_b as a function of the field strength: for smaller values of the ILF-parameter, the binding energy is a growing function of B, whilst for larger α_0 it is a decreasing function of the magnetic field intensity.

This research was partially supported by Colombian Agencies: COLCIENCIAS, CODI-Universidad de Antioquia (Estrategia de Sostenibilidad Grupo de Materia Condensada-UdeA, 2009–2010, 2010–2011), Facultad de Ciencias Exactas y Naturales-Universidad de Antioquia (CAD-exclusive dedication project 2010–2011), and by "El Patrimonio Autónomo Fondo Nacional de Financiamiento para la Ciencia, la Technología y la Innovación Francisco José de Caldas" Contract RC – No. 275-2011.

The work was developed with the help of CENAPAD-SP, Brazil. MEMR acknowledges support from Mexican CONACYT through research grant CB-2008/101777. CAD and MEMR are indebted to COLCIENCIAS and CONACYT for support under the bilateral project "*Estudio de propiedades ópticas y electrónicas en nanoestructuras y sistemas semiconductores de baja dimensión*". The authors are grateful to The Scientific and Technological Research Council of Turkey (TÜBİTAK) for a research grant (TÜBİTAK 109T650).

References

1. K. Goser, P. Glosekotter, J. Dienstuhl, *Nanoelectronics and Nanosystems: From Transistors to Molecular and Quantum Devices* (Springer-Verlag, New York, 2004)
2. C. Weisbuch, B. Vinter, *Quantum Semiconductor Structures: Fundamentals and Applications* (Academic Press, London, 1991)
3. S.D. Ganichev, W. Prettl, *Intense Terahertz Excitation of Semiconductors* (Oxford University Press, Oxford, 2006)
4. A.P. Jauho, K. Johnsen, Phys. Rev. Lett. **76**, 4576 (1996)
5. W. Xu, Europhys. Lett. **40**, 411 (1997)
6. B.G. Enders, F.M.S. Lima, O.A.C. Nunes, A.L.A. Fonseca, D.A. Agrello, Q. Fanyao, E.F. Da Silva Jr., V.N. Freire, Phys. Rev. B **70**, 035307 (2004)
7. R.G. Mani, J.H. Smet, K. von Klitzing, V. Narayanamurti, W.B. Johnson, V. Umansky, Nature **420**, 646 (2002)
8. N.G. Asmar, A.G. Markelz, E.G. Gwinn, J. Cerne, M.S. Sherwin, K.L. Campman, P.F. Hopkins, A.C. Gossard, Phys. Rev. B **51**, 18041 (1995)
9. H. Hsu, L.E. Reichl, Phys. Rev. B **74**, 115406 (2006)
10. L.C.M. Miranda, J. Phys. C: Solid State Phys. **9**, 2971 (1976)
11. O.A.C. Nunes, Solid State Commun. **45**, 53 (1983)
12. R.M.O. Galvao, L.C.M. Miranda, Phys. Rev. B **28**, 3593 (1983)
13. J.W. Sakai, O.A.C. Nunes, Solid State Commun. **64**, 1393 (1987)
14. H.S. Brandi, A. Latgé, L.E. Oliveira, Phys. Stat. Sol. (b) **210**, 671 (1998)
15. H.S. Brandi, A. Latgé, L.E. Oliveira, Phys. Rev. B **70**, 153303 (2004)
16. E.C. Niculescu, L.M. Burileanu, J. Optoelectron Adv. Mater. **9**, 2713 (2007)
17. F.E. López, E. Reyes-Gómez, H.S. Brandi, N. Porras-Montenegro, L.E. Oliveira, J. Phys. D Appl. Phys. **42**, 115304 (2009)
18. E. Kasapoglu, I. Sökmen, Physica B **403**, 3746 (2008)
19. O.O.D. Neto, F. Qu, Superlatt. Microstruct. **35**, 1 (2004)
20. F. Ungan, U. Yesilgul, S. Şakiroglu, E. Kasapoglu, H. Sari, I. Sökmen, Phys. Lett. A **374**, 2980 (2010)
21. E.C. Niculescu, L.M. Burileanu, A. Radu, Superlatt. Microstruct. **44**, 173 (2008)
22. E.C. Niculescu, A. Radu, M. Stafe, Superlatt. Microstruct. **46**, 443 (2009)
23. A.J. Peter, Phys. Lett. A **374**, 2170 (2010)
24. E. Kasapoglu, H. Sari, U. Yesilgul, I Sökmen, J. Phys.: Condens. Matter **18**, 6263 (2006)
25. M. Santhi, A.J. Peter, Eur. Phys. J. B **71**, 225 (2009)
26. C.A. Duque, E. Kasapoglu, S. Şakiroglu, H. Sari, I. Sökmen, Appl. Surface Sci. **256**, 7406 (2010)
27. N. Eseanu, Phys. Lett. A **374**, 1278 (2010)
28. F.M.S. Lima, M.A. Amato, O.A.C. Nunes, A.L.A. Fonseca, B.G. Enders, E.F. da Silva Jr., J. Appl. Phys. **105**, 123111 (2009)
29. L.P. Gorkov, I.E. Dzyaloshinskii, Sov. Phys. J. Exp. Theor. Phys. **26**, 449 (1968)
30. K. Chang, F.M. Peeters, Phys. Rev. B **63**, 153307 (2001)
31. Yu. E. Lozovik, I.V. Ovchinnikov, S. Yu. Volkov, L.V. Butov, D.S. Chemla, Phys. Rev. B **65**, 235304 (2002)
32. A.M. Fox, D.A.B. Miller, G. Livescu, J.E. Cunningham, W.Y. Jan, Phys. Rev. B **44**, 6231 (1991)
33. I. Galbraith, G. Duggan, Phys. Rev. B **40**, 5515 (1989)
34. J.-B. Xia, W.-J. Fan, Phys. Rev. B **40**, 8508 (1989)
35. M. Gavrila, J.Z. Kaminski, Phys. Rev. Lett. **52**, 613 (1984)
36. M. Pont, N.R. Walet, M. Gavrila, C.W. McCurdy, Phys. Rev. Lett. **61**, 939 (1988)
37. H. Sari, E. Kasapoglu, I. Sökmen, Phys. Lett. A **311**, 60 (2003)
38. E. Kasapoglu, H. Sari, M. Güneş, I. Sökmen, Surface Rev. Lett. **11**, 403 (2004)